J. Biochem. **134**, 427–432 (2003)
DOI: 10.1093/jb/mvg160

Structural Elucidation of the Protein- and Membrane-Binding Properties of the N-Terminal Tail Domain of Human Annexin II

Yoon-Hun Hong, Hyung-Sik Won, Hee-Chul Ahn and Bong-Jin Lee*

National Research Laboratory (MPS), College of Pharmacy, Seoul National University, San 56-1, Shillim-Dong, Kwanak-Gu, Seoul 151-742, Korea

Received March 20, 2003; accepted July 5, 2003

The conformational preferences and the solution structure of AnxII^{N31}, a peptide corresponding to the full-length sequence (residues 1–31) of the human annexin II N-terminal tail domain, were investigated by circular dichroism (CD) and nuclear magnetic resonance (NMR) spectroscopy. CD results showed that AnxII^{N31} adopts a mainly α-helical conformation in hydrophobic or membrane-mimetic environments, while a predominantly random structure is adopted in aqueous buffer. In contrast to previous results of the annexin I N-terminal domain peptide [Yoon *et al.* (2000) *FEBS Lett.* 484, 241–245], calcium ions showed no effect on the structure of AnxII^{N31}. The NMR-derived structure of AnxII^{N31} in 50% TFE/water mixture showed a horseshoe-like fold comprising the N-terminal amphipathic α-helix, the following loop, and the C-terminal helical region. Together, the results establish the first detailed structural data on the N-terminal tail domain of annexin II, and suggest the possibility of the domain to undergo Ca^{2+}-independent membrane-binding.

Key words: annexin II, AnxII^{N31}, CD, NMR, N-terminal tail domain.

Abbreviations: AnxII^{N31}, peptide corresponding to residues 1 to 31 of human annexin II; CD, circular dichroism; CSI, chemical shift index; DQF-COSY, double quantum filtered correlation spectroscopy; NMR, nuclear magnetic resonance; NOE, nuclear Overhauser effect; NOESY, NOE spectroscopy; r.m.s.d., root mean square deviation; SDS, sodium dodecyl sulfate; TFE, 2,2,2-trifluoroethanol; TOCSY, total correlation spectroscopy.

Annexins, a family of ubiquitous Ca^{2+} binding proteins, are known to be involved in many important cellular processes such as anti-inflammation, anti-coagulation, membrane trafficking, *etc.* (*1–4*). Typically, all annexins share the characteristic biochemical property of being able to bind to negatively charged phospholipids and cellular membranes in a Ca^{2+}-dependent manner, and some members of the family also interact Ca^{2+}-dependently with certain cytoskeletal elements. In particular, annexin II (AnxII) is thought to play a role in exocytotic and endocytotic processes (*5*, *6*), although its exact physiological function is unclear. The Ca^{2+}-regulated function of AnxII in the exocytotic pathway seems to depend on the formation of a complex between the protein and its intracellular ligand, the S100 protein p11. However, it has been revealed that the association of the AnxII monomer with the endosomal membrane is not regulated by either Ca^{2+}- or p11-binding.

Each annexin is composed of two parts, a major C-terminal core domain and a minor N-terminal tail domain. The similar properties of all annexins regarding Ca^{2+} and phospholipids are displayed by the C-terminal core domains, which contain highly conserved sequences and structures. Unique to the individual members of the annexin family is the N-terminal tail domain, which varies widely in length and sequence. Thus, it has been proposed that the structurally distinct N-terminal domain of each annexin imparts functional specificity (*7–11*). Indeed, many experimental results describing the different functional roles of the N-terminal tail domains have been reported (*12–16*). Particularly, the N-terminal tail of AnxII is involved in at least three types of biochemical reactions that are closely related to its physiological functions. First, the first 12 residues in the AnxII N-terminal tail domain bind to p11, a member of the S100 protein family, resulting in the formation of a heterotetramer, $AnxII_2$-$p11_2$. Second, the AnxII N-terminal tail domain includes phosphorylation sites at positions Ser11, Tyr23, and Ser25. Finally, proteolysis at position 28 results in increased Ca^{2+}-sensitivity of the protein (*17*). Several lines of evidence demonstrate that the N-terminal tail domain of annexin II regulates the Ca^{2+}-dependent membrane binding of the protein (*17–20*). However, no structural evidence has been reported for whether the N-terminal tail of annexin II itself binds to membrane.

Although the 3D structures of more than 10 annexins are presently available (*21–30*), knowledge of the N-terminal domain structure of annexins is very scant because structural studies have been conducted using proteins with short or truncated N-terminal tail domains. The structure of AnxII has been solved for such a truncated protein with the first visible residue Thr 30 (*25*). Although the full-length structure of the AnxII N-terminal tail domain is not yet available, the recently solved crystal structure of the p11-bound peptide corresponding to the N-terminal 12 residues of AnxII shows a helical conformation (*31*). Unfortunately, however, no detailed structure has been reported for the N-terminal tail domain of the p11-free AnxII monomer.

*To whom correspondence should be addressed. Fax: +82-2-872-3632, E-mail: lbj@nmr.snu.ac.kr

In this study, we performed circular dichroism (CD) and nuclear magnetic resonance (NMR) spectroscopy on a p11-free full-length peptide of the AnxII N-terminal tail domain. We report the conformational preferences of the peptide in different solutions, aqueous buffer,a hydrophobic environment, and membrane-mimetic micelles. Additionally, the Ca^{2+}-binding ability of the peptide and the Ca^{2+}-binding effect on the peptide structure in SDS micelles were investigated by CD spectroscopy.

MATERIALS AND METHODS

Materials and Peptide Preparation—$AnxII^{N31}$, the synthetic peptide corresponding to residues 1 to 31 of human annexin II (H_2N-STVHEILCKLSLEGDHSTPPSAYGSV-KAYTN-COOH), was purchased from ANYGEN (Kwangju, Korea; URL, http://www.anygen.com). The sequence and the purity of the peptide were confirmed by mass-spectrometry and high performance liquid chromatography. 2,2,2-trifluroethanol-d_3 99.5% (TFE-d_3) and sodium 4,4-dimethyl-4-silapentane-1-sulfonate (DSS) were obtained from Aldrich. Sodium dodecyl-d_{25} sulfate (SDS-d_{25}) and D_2O 99.95% were obtained from Sigma and Isotec, respectively, and all other chemicals were of analytical grade obtained from various manufacturers.

CD and NMR Spectroscopy—Circular dichroism (CD) spectra were obtained at 293K on a JASCO J-715 spectropolarimeter, using a 2 mm path-length cell with a 1 nm bandwidth, 0.2 nm step resolution, 4 sec response time, and a scan speed of 50 nm/min. Three scans were added and averaged, and then the CD signal of the solvent was subtracted. Samples were prepared by dissolving the peptide powder in various solvents: 50 mM potassium phosphate buffer (pH 6.5), TFE/H_2O mixtures, and 10 mM SDS. Calcium ions were added from a stock solution of 150 mM $CaCl_2$. Samples for nuclear magnetic resonance (NMR) measurements contained 3 mM peptide in TFE-d_3/H_2O (1:1, v/v) at pH 4.0, and in 300 mM SDS-d_{25} at pH 4.0. All NMR spectra were recorded at 298K on Bruker DRX-500 and 600 spectrometers equipped with a gradient unit. The 2D TOCSY and NOESY spectra were acquired with mixing times of 60 ms and 200 ms, respectively. The WATERGATE sequence (*32*) was used to suppress the solvent signals in the NOESY and TOCSY experiments. For the DQF-COSY experiments, solvent suppression was achieved using selective low-power irradiation of the water resonance. All NMR spectra were processed and analyzed using NMRPipe/NMRDraw software and the NMRView program (*33*, *34*). For CSI prediction, chemical shifts were referenced to DSS by the method and reference values of Wishart *et al*. (*35*).

Resonance Assignments and Structure Calculation—Sequence-specific assignments of the proton resonances were achieved by spin system identification from TOCSY and DQF-COSY spectra, followed by sequential assignments through NOE connectivities (*36*). Distance restraints were obtained from the NOESY spectra. NOE data from the NOESY spectra were classified into three classes, strong, medium, and weak, corresponding to upper bound interproton distance restraints of 3.0, 4.0, and 5.0 Å, respectively. Lower distance bounds were taken as the sum of the van der Waals radii of 1.8 Å. Pseudoatom corrections were applied to non-specifically assigned methylene, methyl, and aromatic ring protons (*36*). For the structure calculation, a total of 364 distance restraints were achieved: 114 intra-residue, 127 sequential, 119 medium-range [from *i*th to (*i*+2)th, (*i*+3)th and and (*i*+4)th residues], and 4 long-range [*i*th to (*i*+5)th] NOEs. Then, the 3D structures were calculated using the simulated annealing and energy minimization protocol in the program XPLOR 3.851 (*37*) as described previously (*38*, *39*). Out of the initially calculated 50 structures, 30 with no distance violation larger than 0.5 Å were selected for refinement. Then, of the refined 30 structures, 15 structures with the lowest energies were finally chosen to represent the solution structure of $AnxII^{N31}$.

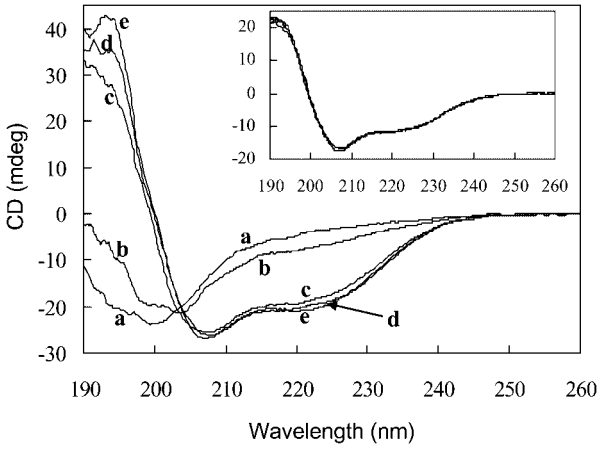

Fig. 1. **CD spectra of 33 μM $AnxII^{N31}$ in 50 mM potassium phosphate buffer (line a) and in TFE/water mixtures (line b, 10%; c, 30%; d, 50%; e, 70% TFE).** Inset shows the superimposed CD spectra of 24 μM $AnxII^{N31}$ in 10 mM SDS micelles in the absence and in the presence of 1, 3, and 5 molar equivalents of calcium ions.

RESULTS

Conformational Preferences of $AnxII^{N31}$—The conformational preferences of $AnxII^{N31}$ in different solvent environments were investigated by CD spectroscopy (Fig. 1). In aqueous buffer, the CD spectrum of $AnxII^{N31}$ showed a strong negative band at 200 nm, indicating a predominantly random-coil conformation. However, in TFE/H_2O mixtures, the CD spectra showed a positive band at 193 nm and double minima at 208 and 222 nm, which are indicative of a highly α-helical conformation (*38–41*). The signals at 193, 208, and 222 nm were intensified by increasing concentrations of TFE, which indicates that the helicity of the peptide is increased in more hydrophobic environments. The spectral change induced by increased concentrations of TFE was nearly complete at about 50% TFE/water, and no significant spectral change occurred when the pH was varied from 3.0 to 7.0 in this solution (data not shown). The CD spectrum of $AnxII^{N31}$ in 10 mM SDS, which is above the critical micellar concentration of SDS (*42*), also showed a typical α-helix pattern, and showed no significant change upon the addition of Ca^{2+} up to 5 molar equivalents (Fig. 1).

NMR Structures of $AnxII^{N31}$—The helical structure of $AnxII^{N31}$ in TFE/water was investigated by NMR spectroscopy. Table 1 lists the nearly complete assignments of

Table 1. **H chemical shifts (ppm) of AnxII^{N31} in 50% TFE, at pH 4.0 and 298K.**

	H^N	Hα	Hβ	Others
S1		4.36	4.01/3.93	
T2	8.43	4.44	4.36	$H\gamma^2$ 1.24
V3	8.24	3.70	1.93	Hγ (0.96/0.83)
H4	7.82	4.25	3.19	$H\delta^2/\varepsilon^1$ 7.14/8.36
E5	7.72	3.85	2.24/2.10	Hγ (2.51/2.40)
I6	7.89	3.63	1.92	$H\gamma^1$ (1.64/1.10); $H\gamma^2/\delta$ 0.85/0.76
L7	8.28	4.03	1.81/1.40	Hγ/δ 1.81/0.77
C8	8.10	4.38	3.07/2.88	
K9	8.17	3.95	1.94	Hγ (1.52/1.33); Hδ/ε 1.61/2.88
L10	8.57	4.04	1.80/1.43	Hγ/δ 1.80/ 0.77
S11	8.00	4.19	4.03/3.91	
L12	7.82	4.17	1.77/1.55	Hγ 1.77
E13	8.00	4.18	2.11	Hγ 2.51/2.41
G14	8.02	3.92/3.84		
D15	7.88	4.58	2.76	
H16	8.23	4.73	3.34/3.15	$H\delta^2/\varepsilon^1$ 7.15/8.47
S17	8.14	4.48	3.85	
T18	7.92	4.58	4.11	$H\gamma^2$ 1.17
P19		4.39	2.28/1.90	Hγ (2.01/1.94); Hδ (3.82/3.60)
P20		4.29	2.22/1.87	Hγ 1.99; Hδ (3.75/3.58)
S21	7.80	4.30	3.87/3.77	
A22	8.04	4.20	1.25	
Y23	7.71	4.36	3.01/2.91	Hδ/ε 7.02/6.74
G24	8.00	3.87/3.79		
S25	7.83	4.39	3.90/3.82	
V26	7.79	3.99	2.07	Hγ (0.91/0.88)
K27	7.94	4.18	1.70/1.62	Hγ 1.33
A28	7.79	4.17	1.24	
Y29	7.71	4.52	2.93/3.07	Hδ/ε 7.05/6.75
T30	7.55	4.30	4.20	$H\gamma^2$ 1.13
N31	7.84	4.54	2.76/2.71	

the proton chemical shifts of AnxII^{N31} in 50% TFE/water. As shown in Fig. 2, the presence of a typical α-helix from V3 to E13 is supported in TFE/water by the well ordered NOE connectivities of $d_{NN}(i,i+1)$, $d_{NN}(i,i+2)$, $d\alpha\beta(i,i+3)$, $d\alpha_N(i,i+3)$ and $d\alpha_N(i,i+4)$, as well as by the Hα CSI values indicating helical propensity. The Hα CSI results indicate another helical structure in the C-terminal region comprising residues P20–A28. However, the helical NOE connectivities in this region are less frequently observed. This indicates that the C-terminal helical structure of AnxII^{N31} in TFE/water is probably less stabilized than its N-terminal helix, and thus somewhat loosened.

A highly refined three-dimensional structure of AnxII^{N31} in TFE/water could not be obtained, mainly due to the deficiency of unambiguous restraints. However, as shown in Fig. 3, the NOE-based and energy-minimized backbone structures of AnxII^{N31} in TFE/water showed a reasonable fold with a horseshoe-like shape. The overall structure was folded into an α-helix spanning from Val 3 to Glu 13, the following loop region, and the C-terminal helical region. The N-terminal region from Val 3 to Glu 13 adopted a well-ordered and highly stabilized α-helix. This helix exhibits typical amphipathic characteristics, positioning the hydrophobic residues on one side and the hydrophilic residues on the other side of the helical axis (Fig. 3C). The helical length and the amphipathic property of the N-terminal α-helix are consistent with those observed in the p11-bound AnxII N-terminal peptide (*31*). Short helical structures were fractionally observed in the C-terminal region, mainly in residues S21-Y23 and

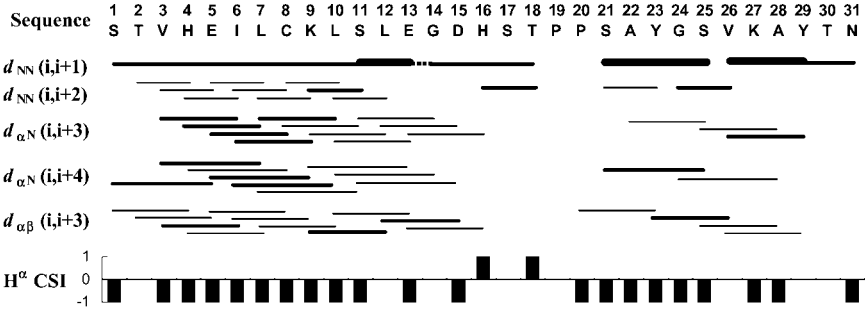

Fig. 2. **Overview of the NOE connectivities and $^1H\alpha$ CSI results of AnxII^{N31} in a 50% TFE/water mixture.** For the NOE connectivity data, the height of the bar corresponds to the intensity of the correlation (weak, medium, or strong). The dotted line represents a tentative assignment due to spectral overlap.

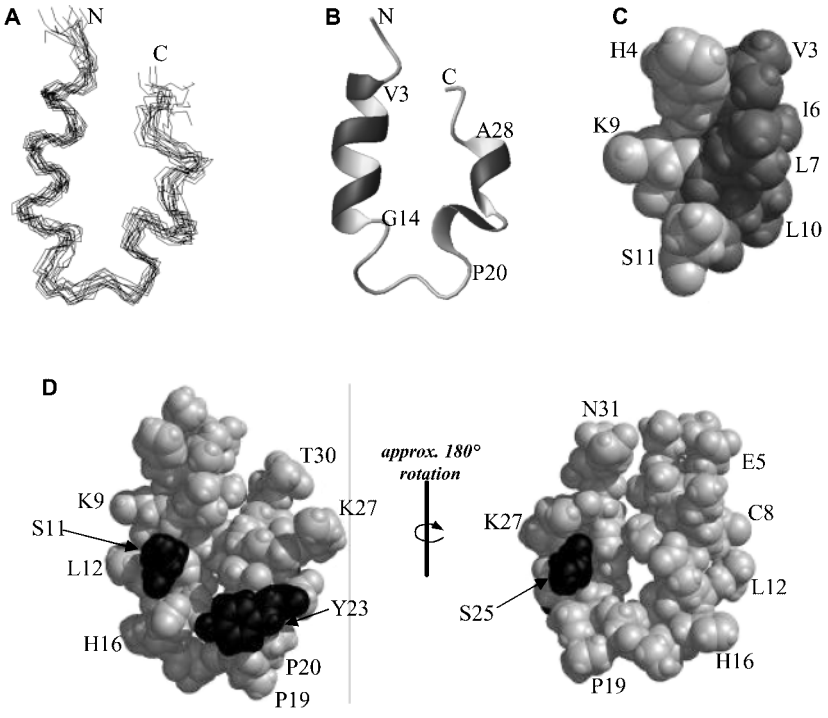

Fig. 3. **NMR structures of AnxII^{N31} in 50% TFE/water.** Backbone atoms (N, Cα, and C′) of the finally selected 15 structures are superimposed in panel A. Their refined average structure is depicted as a ribbon diagram in panel B. Residues 3–11 of the refined average structure are enlarged as a conic representation in panel C, in which hydrophobic and hydrophilic residues are shown in dark gray and light gray, respectively. Conic representations of the entire sequence are shown in panel D, with the phosphorylation sites (residues 11, 23, and 25) shown in black.

S25-A28. These helical fragments are kinked or adopt a 3_{10}-helix conformation in most of the calculated structures. Thus, the structures in Fig. 3 indicate that the C-terminal region of AnxII^{N31} in TFE/water adopts a partially ordered helical conformation. The relatively destabilized helical conformation in this C-terminal region may be attributable to the break in the peptide bond at position 31. The structure in the inter-helical hinge region comprising residues G14-P20 adopt a helix-like loop, which allows close proximity between the N-terminal α-helix and the C-terminal helical region. This horseshoe-like fold of AnxII^{N31} apparently seems to contain interactions between side-chains of the N-terminal and the C-terminal helical parts. Particularly, the hydrophobic side of the N-terminal helix, which interacts with p11, faces toward the C-terminal helical region. Unfortunately, however, long-rage NOEs could not be ensured between the two helical stretches, due to severe spectral overlap. However, the structural origin of the horseshoe-like fold can be supported by a few long-range NOEs detected between the Thr18 and Tyr23 side chains. Especially, Pro19 and Pro20 residues, with a *trans*-conformation, would be expected to dominate the relative orientation between the N-terminal helix and the C-terminal helical region of AnxII^{N31}.

We have previously solved the three-dimensional structure of the annexin I N-terminal tail domain (AnxI^{N26}) in SDS micelles (*39*). Unfortunately, in the present work, the quality of the NMR spectra of AnxII^{N31} in SDS micelles was too low to analyze the peptide structure in this solution (data not shown) due to low sensitivity, severe peak broadening and overlap. However, the remarkable peak broadening in the NMR spectra of AnxII^{N31} in SDS micelles indicates that the peptide probably associated with the SDS micelle, resulting in a large molecular weight complex system.

DISCUSSION

The crystal structure of p11 in complex with the AnxII N-terminal 12-residue peptide has revealed that the peptide adopts an α-helical conformation in its p11-bound state (*31*). However, this helical conformation seems to be induced upon its binding to p11, probably by the hydrophobic environment in the binding pocket. The present CD results (Fig. 1) indicate that the annexin II N-terminal peptide has no inherent propensity for an ordered structure in aqueous solution, while it can adopt a helical conformation in TFE/water mixtures. The NMR structure of AnxII^{N31} in TFE/water mixture (Fig. 3) clearly conforms with its amphipathic property and the length of the AnxII^{N31} N-terminal helix is consistent with that observed in the p11-bound crystal structure of the N-terminal 12-residue peptide. TFE, either neat or mixed with water, is a representative medium typically used to mimic the hydrophobic environments of peptide binding sites in proteins (*43*). Thus, the conformational transition of AnxII^{N31} from random-coil in aqueous solution to α-helix in TFE/water mixtures can be interpreted as an induced-fit process of the peptide in the binding site of p11. Nevertheless, the overall fold of AnxII^{N31} in TFE/water mixture (Fig. 3) does not seem to reflect the p11-bound state. In the crystal structure of the AnxII peptide-p11 complex, the peptide binding is driven by hydrophobic interactions. In contrast, in the present NMR structure, the hydrophobic side of the N-terminal amphipathic helix faces the C-terminal helical region. Although direct contact between the N-terminal α-helix and the C-terminal helical region could not be demonstrated, the horseshoe-like backbone geometry allows the close proximity between the two regions. This conformation would not be expected to assume the hydrophobic contact observed in the crystal structure, since the hydrophobic face of the N-

terminal helix would be masked by the C-terminal helical region. Instead, the horseshoe-like fold of AnxII^{N31} orients the N-terminus in the same direction as the C-terminus, *i.e.*, toward the core domain expected in the intact form. Thus, it is reasonable to conclude that the 3-dimensional fold of AnxII^{N31} in TFE/water mixtures reflects the conformation in intact AnxII. In the case of annexin I, the N-terminal tail domain has been strongly suggested to interact with the core domain in its intact form (*44*). Likewise, the N-terminal tail domain in intact AnxII can be expected to adopt a helical conformation with a horseshoe-like fold naturally during its autonomous folding process in aqueous solution, either by a direct interaction with the C-terminal core domain or due to the hydrophobic environment provided by this domain. Then, the horseshoe-like fold would change to expose the N-terminal hydrophobic side by interacting with p11. The inter-helical hinge region in the present AnxII^{N31} structure does not adopted an ordered structure and has two sequentially linked prolines, an amino acid that along with glycine is known to allow the most diverse backbone geometry in proteins. In addition, since the inter-helical hinge region itself is probably flexible, as supported by the poor appearance of inter-residue NOEs in this region (Fig. 2), it would allow an alteration in the relative orientation between the N-terminal amphipathic α-helix and the C-terminal helical region. The horseshoe-like fold of the AnxII^{N31} has another characteristic related to its function. The N-terminal tail domain of annexin II contains three phosphorylation sites (Ser11, Tyr23, and Ser25), and phosphorylation plays important roles in the diverse functions of annexin II. As shown in Fig 3, the horseshoe-like fold allows all three residues to expose their side-chains to the solvent-accessible surface. This orientation would make the phosphorylation process easy in the intact form.

The amphipathic helical conformation, which has been observed for many membrane-interacting peptides including the N-terminal domain of annexin I, is known to be an important factor for interaction with membranes (*38–40*). In the present results, the N-terminal region of AnxII^{N31} also shows a typical amphipathic α-helical conformation, implying the potential for membrane interaction. The membrane-interacting possibility of the AnxII N-terminal tail domain can be inferred from the following recently reported investigations. Tyrosine phosphorylation at this domain in the $AxnII_2$-$p11_2$ tetramer is stimulated by protein-membrane association (*6*). The association of AnxII with the endosomal membrane is independent of both complex formation with p11 and Ca^{2+}, but deletion of the N-terminal tail abolishes the association of the protein with endosomes (*5*). The present CD results showing of AnxII^{N31} adopting a helical conformation in SDS micelles also support the membrane binding property of the AnxII N-terminal tail domain, since SDS micelles with negatively charged surfaces mimic the negatively charged phospholipid membrane where annexins bind (*39*, *45*). This conformational behavior of AnxII^{N31} is common to many membrane-binding peptides (*39–41*, *46–50*). Based on the present CD results, in which Ca^{2+} has no effect on the structure of AnxII^{N31}, the N-terminal tail domain of annexin II could interact with the membrane in a Ca^{2+}-independent manner. In contrast, our previous CD results on the N-terminal tail peptide of human annexin I (*39*) showed that Ca^{2+} significantly stabilizes the helical structure of the peptide. In addition, from the structural investigation by NMR, the negatively charged Glu-rich region could represent a putative Ca^{2+}-binding site in the N-terminal tail domain of annexin I. This difference in Ca^{2+}-binding properties between the N-terminal tails of annexin I and annexin II may be related to their functional specificities in the regulation of membrane interactions.

This work was supported by the National Research Laboratory Program (M1-0203-00-0075) from the Korean Institute of Science & Technology, Evaluation and Planning, Republic of Korea. This work was also supported in part by the 2002 BK21 project for Medicine, Dentistry, and Pharmacy.

REFERENCES

1. Creutz, C.E. (1992) The annexins and exocytosis. *Science* **258**, 924–931
2. Raynal, P. and Pollard, H.B. (1994) Annexins: the problem of assessing the biological role for a gene family of multifunctional calcium- and phospholipids-binding proteins. *Biochim. Biophys. Acta* **1197**, 63–93
3. Swairjo, M.A. and Seaton, B.A. (1994) Annexin structure and membrane interactions: a molecular perspective. *Annu. Rev. Biophys Biomol. Struct.* **23**, 193–213
4. Gerke, V. and Moss, S.E. (1997) Annexins and membrane dynamics. *Biochim. Biophys. Acta* **1357**, 129–154
5. Jost, M., Zeuschner, D., Seemann, J., Weber, K., and Gerke, V. (1997) Identification and characterization of a novel type of annexin-membrane interaction: Ca^{2+} is not required for the association of annexin II with early endosomes. *J. Cell Sci.* **110**, 221–228
6. Bellagamba, C., Hubaishy, I., Bjorge, J.D., Fitzpatrick, S.L., Fujita, D.J., and Waisman, D.M. (1997) Tyrosine phosphorylation of annexin II tetramer is stimulated by membrane binding. *J. Biol. Chem.* **272**, 3195–3199
7. Han, H.-Y., Oh, J.-Y., Na, D.-S., and Lee, B.-J. (1998) NMR analyses of the interactions of human annexin I with ATP, Ca^{2+}, and Mg^{2+}. *FEBS Lett.* **425**, 523–527
8. Mailliard, W.S., Haigler, H.T., and Schlaepfer, D.D. (1996) Calcium-dependent binding of S100C to the N-terminal domain of annexin I. *J. Biol. Chem.* **271**, 719–725
9. Walther, A., Riehemann, K., and Gerke, V. (2000) A novel ligand of the formyl peptide receptor: annexin I regulates neutrophil extravasation by interacting with the FPR. *Mol. Cell* **5**, 831–840
10. Arboledas, D., Olmo, N., Lizarbe, M.A., and Turnay, J. (1998) Role of the N-terminus in the structure and stability of chicken annexin V. *FEBS Lett.* **416**, 217–220
11. Becker, T., Weber, K., and Johnsson, N. (1990) Protein-protein recognition via short amphiphilic helices; a mutational analysis of the binding site of annexin II for p11. *EMBO J.* **9**, 4207–4213
12. Rosengarth, A., Wintergalen, A., Galla, H.J., Hinz, H.J., and Gerke, V. (1998) Ca^{2+}-independent interaction of annexin I with phospholipid monolayers. *FEBS Lett.* **438**, 279–284
13. Hoekstra, D., Buist-Arkema, R., Klappe, K., and Reutelingsperger, C.P. (1993) Interaction of annexins with membranes: the N-terminus as a governing parameter as revealed with a chimeric annexin. *Biochemistry* **32**, 14194–14202
14. Liu, L., Fisher, A.B., and Zimmerman, U.J. (1995) Regulation of annexin I by proteolysis in rat alveolar epithelial type II cells. *Biochem. Mol. Biol. Int.* **36**, 373–381
15. Ando, Y., Imamura, S., Hong, Y.M., Owada, M.K., Kakunaga, T., and Kannagi, R. (1989) Enhancement of calcium sensitivity of lipocortin I in phospholipid binding induced by limited proteolysis and phosphorylation at the amino terminus as ana-

lyzed by phospholipid affinity column chromatography. *J. Biol. Chem.* **264**, 6948–6955
16. Wang, W. and Creutz, C.E. (1994) Role of the amino-terminal domain in regulating interactions of annexin I with membranes: effects of amino-terminal truncation and mutagenesis of the phosphorylation sites. *Biochemistry* **33**, 275–282
17. Drust, D.S. and Creutz, C.E. (1988) Aggregation of chromaffin granules by calpactin at micromolar levels of calcium. *Nature* **331**, 88–91
18. Glenney, J.R. (1986) Phospholipid-dependent Ca^{2+}-binding by the 36-kDa tyrosine kinase substrate (calpactin) and its 33-kDa core. *J. Biol. Chem.* **261**, 7247–7252
19. Powell, M.A. and Glenney, J.R. (1987) Regulation of calpactin I phospholipid binding by calpactin I light-chain binding and phosphorylation by p60v-src. *Biochem. J.* **247**, 321–328
20. Ayala-Sanmartin, J., Gouache, P., and Henry, J.P. (2000) N-Terminal domain of annexin 2 regulates Ca^{2+}-dependent membrane aggregation by the core domain: a site directed mutagenesis study. *Biochemistry* **39**, 15190–15198
21. Favier-Perron, B., Lewit-Bentley, A., and Russo-Marie, F. (1996) The high-resolution crystal structure of human annexin III shows subtle differences with annexin V. *Biochemistry* **35**, 1740–1744
22. Hofmann, A., Proust, J., Dorowski, A., Schantz, R., and Huber, R. (2000) Annexin 24 from Capsicum annuum. X-ray structure and biochemical characterization. *J. Biol. Chem.* **275**, 8072–8082
23. Weng, X., Luecke, H., Song, I.S., Kang, D.S., Kim, S.H., and Huber, R. (1993) Crystal structure of human annexin I at 2.5 Å resolution. *Protein Sci.* **2**, 448–458
24. Burger, A., Berendes, R., Liemann, S., Benz, J., Hofmann, A., Göttig, P., Huber, R., Gerke, V., Thiel, C., Romisch, J., and Weber, K. (1996) The crystal structure and ion channel activity of human annexin II, a peripheral membrane protein. *J. Mol. Biol.* **257**, 839–847
25. Gao, J., Li, Y., and Yan, H. (1999) NMR solution structure of domain 1 of human annexin I shows an autonomous folding unit. *J. Biol. Chem.* **274**, 2971–2977
26. Zanotti, G., Malpeli, G., Gliubich, F., Folli, C., Stoppini, M., Olivi, L., Savoia, A., and Berni, R. (1998) Structure of the trigonal crystal form of bovine annexin IV. *Biochem. J.* **329**, 101–106
27. Sopkova, J., Renouard, M., and Lewit-Bentley, A. (1993) The crystal structure of a new high-calcium form of annexin V. *J. Mol. Biol.* **234**, 816–825
28. Benz, J., Bergner, A., Hofmann, A., Demange, P., Gottig, P., Liemann, S., Huber, R., and Voges, D. (1996) The structure of recombinant human annexin VI in crystals and membrane-bound. *J. Mol. Biol.* **260**, 638–643
29. Liemann, S., Bringemeier, I., Benz, J., Gottig, P., Hofmann, A., Huber, R., Noegel, A.A., and Jacob, U. (1997) Crystal structure of the C-terminal tetrad repeat from synexin (annexin VII) of Dictyostelium discoideum. *J. Mol. Biol.* **270**, 79–88
30. Luecke, H., Chang, B.T., Mailliard, W.S., Schlaepfer, D.D., and Haigler, H.T. (1995) Crystal structure of the annexin XII hexamer and implications for bilayer insertion. *Nature* **378**, 512–515
31. Rety, S., Sopkova, J., Renouard, M., Osterloh, D., Gerke, V., Tabaries, S., Russo-Marie, F., and Lewit-Bentley, A. (1999) The crystal structure of a complex of p11 with the annexin II N-terminal peptide. *Nat. Struct. Biol.* **6**, 89–95
32. Piotto, M., Saudek, V., and Sklenar, V. (1992) Gradient-tailored excitation for single-quantum NMR spectroscopy of aqueous solutions. *J. Biomol. NMR* **2**, 661–666
33. Delaglio, F., Grzesiek, S., Vuister, G.W., Zhu, G., Pfeifer, J., and Bax, A. (1995) NMRPipe: a multidimensional spectral processing system based on UNIX pipes. *J. Biomol. NMR* **6**, 277–293
34. Johnson, B.A. and Blevins, R.A. (1994) NMRView: a computer program for the visualization and analysis of NMR data. *J. Biomol. NMR* **4**, 603–614
35. Wishart, D.S., Sykes, B.D., and Richards, F.M. (1992) The Chemical Shift Index: A Fast and Simple Method for the Assignment of Protein Secondary Structure through NMR Spectroscopy. *Biochemistry* **31**, 1647–1651
36. Wüthrich, K. (1986) *NMR of Protein and Nucleic Acids*, John Wiley and Sons, New York
37. Brüger, A.T. (1992) *XPLOR 3.1. A System for X-Ray Crystallography and NMR*, Yale University Press, New Haven, CT
38. Park, S.H., Kim, Y.K., Park, J.W., Lee, B., and Lee, B.J. (2000) Solution structure of the antimicrobial peptide gaegurin 4 by ^{1}H and ^{15}N nuclear magnetic resonance spectroscopy. *Eur. J. Biochem.* **267**, 2695–2704
39. Yoon, M.-K., Park, S.-H., Won, H.-S., Na, D.-S., and Lee, B.-J. (2000) Solution structure and membrane-binding property of the N-terminal tail domain of human annexin I. *FEBS Lett.* **484**, 241–245
40. Gilbert, G.E. and Baleja, J.D. (1995) Membrane-binding peptide from the C2 domain of factor VIII forms an amphipathic structure as determined by NMR spectroscopy. *Biochemistry* **34**, 3022–3031
41. Lancelin, J.M., Bally, I., Arlaud, G.J., Blackledge, M., Gans, P., Stein, M., and Jacquot, J.P. (1994) NMR structures of ferredoxin chloroplastic transit peptide from Chlamydomonas reinhardtii promoted by trifluoroethanol in aqueous solution. *FEBS Lett.* **343**, 261–266
42. Tessari, M., Foffani, M.T., Mammi, S., and Peggion, E. (1993) Conformation and interactions of uteroglobin fragments 4–14 and 49–65 in aqueous solution containing surfactant micelles. *Biopolymers* **33**, 1877–1887
43. Saviano, G., Crescenzi, O., Picone, D., Temussi, P., and Tancredi, T. (1999) Solution structure of human beta-endorphin in helicogenic solvents: an NMR study. *J. Pept. Sci.* **5**, 410–422
44. Porte, F., de Santa Barbara, P., Phalipou, S., Liautard, J.P., and Widada, J.S. (1997) Change in the N-terminal domain conformation of annexin I that correlates with liposome aggregation is impaired by Ser-27 to Glu mutation that mimics phosphorylation. *Biochim. Biophys. Acta* **1293**, 177–184
45. Wang, G., Treleaven, W.D., and Cushley, R.J. (1996) Conformation of human serum apolipoprotein A-I(166–185) in the presence of sodium dodecyl sulfate or dodecylphosphocholine by ^{1}H-NMR and CD: evidence for specific peptide-SDS interactions. *Biochim. Biophys. Acta* **1301**, 174–184
46. Wienk, H.L., Czisch, M., and de Kruijff, B. (1999) The structural flexibility of the preferredoxin transit peptide. *FEBS Lett.* **453**, 318–326
47. Wray, V., Mertins, D., Kiess, M., Henklein, P., Trowitzsch-Kienast, W., and Schubert, U. (1998) Solution structure of the cytoplasmic domain of the human CD4 glycoprotein by CD and ^{1}H NMR spectroscopy: implications for biological functions. *Biochemistry* **37**, 8527–8538
48. Pfänder, R., Neumann, L., Zweckstetter, M., Seger, C., Holak, T.A., and Tampé, R. (1999) Structure of the active domain of the herpes simplex virus protein ICP47 in water/sodium dodecyl sulfate solution determined by nuclear magnetic resonance spectroscopy. *Biochemistry* **38**, 13692–13698
49. Rizo, J., Blanco, F.J., Kobe, B., Bruch, M.D., and Gierasch, L.M. (1993) Conformational behavior of Escherichia coli OmpA signal peptides in membrane mimetic environments. *Biochemistry* **32**, 4881–4894
50. Chupin, V., Killian, J.A., Breg, J., de Jongh, H.H., Boelens, R., Kaptein, R., and de Kruijff, B. (1995) PhoE signal peptide inserts into micelles as a dynamic helix-break-helix structure, which is modulated by the environment. A two-dimensional ^{1}H NMR study. *Biochemistry* **34**, 11617–11624